

Structural, macro- and micro-mechanical properties of supramolecular bi-component L-Lysine-sodium tetraphenyl borate based hydrogels

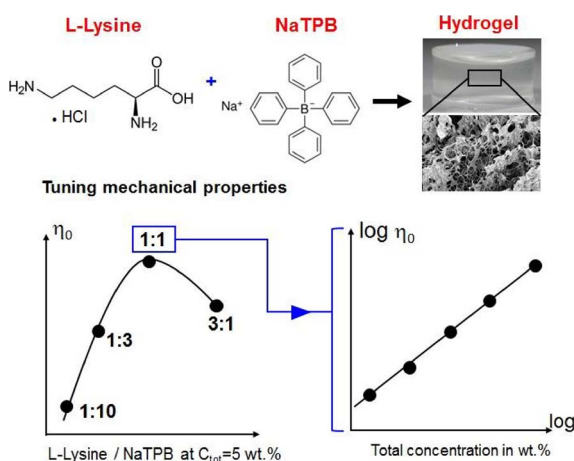
Umair Ahmed Khan^{a,b,*}, Claude Oelschlaeger^b, Firdous Imran Ali^a, Johanna Roether^b, Norbert Willenbacher^b, Imran Ali Hashmi^a

^a Department of Chemistry, University of Karachi, Karachi, Pakistan

^b Karlsruhe Institute for Technology (KIT), Institute for Mechanical Process Engineering and Mechanics, Karlsruhe, Germany



GRAPHICAL ABSTRACT



ARTICLE INFO

Keywords:

Supramolecular self-assemblies
Amino acid based gel
Hydrogels
Rheology
Microrheology

ABSTRACT

We present a new system of bi-component hydrogels formed of L-lysine hydrochloride mixed with sodium tetraphenyl borate with unusual viscoelastic properties which might be useful in tissue engineering, nano-particles synthesis or bioseparation. Beside cationic-anionic molecular interactions, ¹H-NMR experiments have also shown the presence of π -electrons cloud interactions as well as hydrogen bonds stabilizing the supramolecular structure. Bulk rheological and mechanical properties have been characterized using steady and oscillatory shear rheometry as well as uniaxial compression tests. Microstructural information has been deduced from multi particle tracking (MPT) optical microrheology and cryo-preparation scanning electron microscopy (SEM). These gels are shear thickening at low concentrations and shear thinning at higher gelator concentration. Shear and Young's modulus data obtained from different techniques agree fairly well. Zero shear viscosity as well as modulus data obtained for gels with equimolar lysine and borate concentration exhibit concentration dependence $\eta_0 \sim c^{5 \pm 0.5}$ and $G_0 \sim c^{3.4 \pm 0.35}$, respectively. The scaling exponent for η_0 agrees well with predictions for neutral polymer in theta solvent or wormlike micelles in the slow breaking regime whereas the variation in G_0 is unexpectedly high. We attribute this to the unique microstructure consisting of a cellular structure composed of thin sheets connected by tiny fibers. At low concentrations the mesh size of this structure is about 10 μm and fiber diameter increases from ~ 200 nm to ~ 2 μm , only at the highest gelator concentration of 7 wt.% the mesh

* Corresponding author at: Department of Chemistry, University of Karachi, Karachi, Pakistan.
E-mail address: umairosms205@gmail.com (U.A. Khan).

<https://doi.org/10.1016/j.colsurfa.2018.02.068>

Received 15 December 2017; Received in revised form 8 February 2018; Accepted 27 February 2018

Available online 04 March 2018

0927-7757/ © 2018 Elsevier B.V. All rights reserved.

size shrinks to $\sim 5\ \mu\text{m}$ and the fiber diameter to $\sim 400\ \text{nm}$. Consistently, tracer particles in low concentrated gels diffuse freely in an aqueous environment. At higher gelator concentration, however, gelation takes place so fast that tracers are trapped in the elastic sheets / fibrous regions and the modulus G_{MPT} agrees fairly well with bulk data. Varying the molar ratio of both gel-forming components results in a pronounced viscosity maximum at fixed total gelator concentration. Corresponding microstructural changes could again be visualized using cryo-SEM consistent with MPT data. At high lysine fraction, a coarse coral reef type sheet structure is found while at low lysine to borate ratio a network of thick struts is formed. Finally, diffusing wave spectroscopy experiments performed on samples with different lysine to borate ratio revealed that the plateau modulus G_0 is almost independent of temperature whereas the relaxation time T_R becomes faster as temperature increases.

1. Introduction

Spontaneous supramolecular self-assembly of molecules to furnish ordered aggregates is an ever-present phenomena of life observed in pairing of nucleic bases in DNA, RNA, lipid bilayers and proteins (self-assembled polypeptide chains). Supramolecular self-assembly happens due to non-covalent interactions (e.g. Van der Waals and Coulombic interactions, hydrogen bonds, ionic bonds) and has major impact on a range of fields including advanced biological and material sciences due to their characteristic features like thermoreversibility, flexibility in design, experimental convenience, easy tuning in properties etc.

Large polymeric molecules self-assemble into complex DNA or RNA structures based upon supramolecular non-covalent interactions, beyond some of these assemblies can arrest into bulk gel structure [1]. A functional moiety is required which can provide sequential forces for molecules to self-assemble in a well-defined nano-structure [2]. Besides that low molecular weight gels (LMG), composed of small organic molecules are reported in literature. A variety of self-assembled nano-architectures gained attention of material scientists, as their morphology and mechanical properties facilitate new design concepts in tissue engineering [3], drug delivery [4,5], nanomaterials synthesis [6] and electronic device construction [7]. Usually LMG are mechanically not as robust as chemically crosslinked polymeric gels, but morphology and rheology can be tuned in a broad range. Weak non-covalent interaction holds the nano-architecture to a certain stress limit and may self-recover after deformation [8], also LMG may be thermo-responsive [9]. In other words, they are found to be responsive to external stimuli like stress or temperature.

The LMG class in which two molecules interact via non-covalent interactions induced by their functional group moiety and self-assemble to immobilize solvent (water) is known as bi-component low molecular weight hydro-Gelators (Bi-LMHGs). The most common bi-component gelation systems in which both components independently cannot form a gel [10] have been reviewed in detail by Hirts and Smith. Among these systems, gelation via salts from organic acids and bases reveals the role of ionic interactions. Dastidar and coworkers have contributed intensively to this topic and developed soft materials such as supramolecular gels from different organic salts [11–15]. For example, they report that new organo gels can be derived from salts of a primary amine and various derivatives of cinnamic acid [14] or imidazole with dicarboxylic acid [15]. Another successful example of property-based design is the development of low molecular weight gelators via adding CO_2 in an amine solution, which has inspired Weiss and coworkers [16]

as well as Jessop and coworker [17] to develop CO_2 responsive gelators. It has also been reported that cationic surfactant cetyltrimethylammonium bromide (CTAB) upon addition of sodium salicylate furnish hydro gels [18].

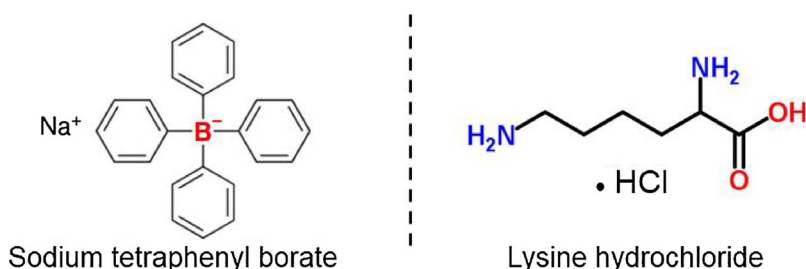
The present study comprises hitherto unreported Bi-LMHGs chemical composition i.e. a biocompatible, biodegradable and environment friendly cation [19] L-lysine hydrochloride (L-LHC) and a conventional amphiphilic anion sodium tetraphenyl borate (NaTPB) (Scheme 1). Derivatives of L-LHC [20] and L-LHC with other surfactant molecules [21] that promote gelation are also reported in literature but the use of L-LHC alone has not been documented so far. NaTPB is usually used to precipitate polycations [22]. Kanato et al. used NaTPB anion to separate ϵ -Poly-L-lysine from culture broth [19]. NaTPB has also been utilized to remove chloride ion from the system and to induce forced gelation [23]. This bi-component system does not require expensive and temperatures sensitive chemicals for gelation like F-moc amino acids, as reported earlier [24]. NaTPB and L-LHC are commercially available which increases their potential towards bulk use in future applications.

This hydrogel is found to be tunable in morphology and mechanical properties. Most of the tunable gels reported so far are organo gels. Hydrogels are also tunable in morphology and physical properties but this is controlled by co-solvents like DMSO [24] or by blending two hydrogelators [25] or by adding nano-rods [26]. In the present study, we have used a different strategy where we blend two molecules, not capable of gelation alone, to furnish instant gelation at room temperature via supramolecular interactions.

This bi-component system is designed based on molecular interactions as further explained in the text from $^1\text{H-NMR}$ experiments. As L-LHC alone cannot form a gel a counterion is required to enable gelation. We selected NaTPB as it contains π -electrons cloud to promote different types of π interactions, while the negatively charged borate works as a counter ion for L-LHC molecule. This supramolecular interaction leads to formation of nano-architecture which enables gelation.

In the present framework, it is found that by changing the total gelator concentration mechanical properties can varied by more than two orders of magnitude. Modification of morphology is possible by altering the ratio of L-LHC and NaTPB and we describe how non-covalent interactions vary the nano-architecture of the gel and how this controls mechanical response and rheological properties.

For the first time, the multiple particle tracking (MPT) technique is used to characterize microstructural and micromechanical properties of such low molecular weight hydrogels. This technique combined with



Scheme 1. Chemical structure of compounds involved in Bi-component gelation system (a) Sodium Tetraphenyl borate (NaTPB) for π interactions and as an anionic counterpart (red). (b) L-lysine hydrochloride (L-LHC) as zwitterion and counter cationic part (blue). (For interpretation of the references to color in this figure legend, the reader is referred to the web version of this article.)

classical rotational rheometry and scanning electron microscopy images provides valuable insight into gel mechanical and structural properties as a function of the total gelator concentration and mixing ratio of both components. The main motivation is to introduce soft materials that may be used as soft tactile sensors due to their conductivity and response upon stress in soft electronics. Additionally, due to their variety of tunable morphological and physical properties, these bi-component gels may also find applications in nano-material synthesis, tissue engineering or drug delivery.

2. Experimental section

2.1. Materials

Both products L-Lysine hydrochloride 99% (L-LHC) and Sodium Tetrphenyl borate 99% (NaTPB) are commercially available; they were purchased from Merck Millipore (Germany). All sample have been prepared using distilled deionized water (Merck Millipore Deionizer).

2.2. Preparation of LMG Bi-component of L-Lysine and sodium Tetrphenyl borate

The sample solutions were prepared by gently stirring L-Lysine mono hydrochloride and sodium Tetrphenyl borate in deionized water (pH = 7) at a temperature of $\sim 90^\circ\text{C}$ until complete dissolution. After that, mixtures were cool down at room temperature without any stirring where the gelation occurs. The cooling procedure was similar for all gels. Gels of equimolar ratio (L-LHC/NaTPB) at different total concentration ranging from 1.5 to 7 wt.% were prepared as well as gels of different molar ratio (3/1; 1/3 and 1/10) at constant total concentration of 5 wt.%. In all cases, gels do not phase-separated and are stable over several weeks.

2.3. Rotational rheometry

A rotational rheometer Thermo MARS II equipped with a plate-plate measuring cell (diameter 20 mm, attached with sandpaper, gap 2 mm) was used to perform steady as well as small amplitude oscillatory shear experiments covering the frequency range from 0.01 to 100 rad s^{-1} . The sandpaper (grit size 60) was directly fixed on both lower and upper plates of the rheometer using double-side tape to avoid slip effects between the gel and plates. Strain sweep experiments performed prior to frequency sweeps ensure that the strain amplitude used was sufficiently small to provide a linear material response at all investigated frequencies. All measurements were performed at 25°C and a solvent trap was used to avoid evaporation of the solvent.

2.4. Multiple particle tracking based optical microrheology

MPT experiments were performed using an inverted fluorescence microscope (Axio Observer D1, Zeiss), equipped with a Fluar 100 \times , N.A. 1.3, oil-immersion lens. We have tracked the Brownian motion of green fluorescent polystyrene PS microspheres of 0.19 and 0.51 μm diameter (Bangs Laboratories) used as tracer particles. Latter have been added in the liquid (sol) solution at a temperature of 90°C , then the mixture was sonicated for several minutes to ensure a uniform particle distribution throughout the sample. Images of these fluorescent beads were recorded onto a personal computer via a sCMOS camera Zyla X (Andor Technology). Displacements of particle centers were monitored in a $127 \times 127\text{-}\mu\text{m}$ field of view, at a rate of 50 frames/s. Movies of the fluctuating microspheres were analyzed by a custom MPT routine incorporated into the software Image Processing System (Visiometrics iPS) [27] and a self-written Matlab program [28] based on the widely used Crocker and Grier tracking algorithm [29]. Additionally, to perform the statistical analysis and characterize the microstructure heterogeneity we examined the distribution of displacements, known as

Van Hove correlation function [30] and determined the non-Gaussian parameter α [31]. This quantity is zero for a Gaussian distribution, while broader distributions result in larger values of α .

2.5. Mechanical compression testing

Uniaxial compression tests were performed at room temperature using a commercial Texture Analyzer TA.XTplus (Stable Micro System, UK) machine with a 5 kg load cell. All samples investigated had the same cylindrical shape: 10 mm in height. Samples were compressed using a 5 mm diameter stamp up to 80% strain at a compression speed of 0.1 mm/s. The Young's modulus, E , was determined as the initial linear slope of the stress-strain curve. More details about the data processing can be found in Oelschlaeger et al. [32].

2.6. Scanning electron microscopy

Gels were first placed in liquid nitrogen for one hour. Then they were freeze dried during 13 h in a Lyovapor L-300 (BUCHI), till the decrease in weight of samples discontinues. After that, samples were sputter-coated via Titanium, and imaged using an environmental scanning electron microscope (FEI Quanta 650 FEG ESEM). Various positions of the samples were investigated at lower magnification and then zoomed to acquire higher magnification images of gel microstructure.

2.7. Diffusing wave spectroscopy

Diffusing wave spectroscopy (DWS) is an extension of the traditional dynamic light scattering (DLS) technique in which multiple light scattering is analyzed. It is a method that allows for detecting the dynamics of embedded micron sized colloidal particles. Due to the Brownian motion of particles, the detector records the intensity fluctuation from which the intensity autocorrelation function (ICF) $g_2(\tau) - 1 = \langle I(t) \cdot I(t + \tau) \rangle_t / \langle I(t) \rangle_t^2 - 1$ can be calculated, then the mean square displacement (MSD) and finally both viscoelastic moduli $G'(\omega)$ and $G''(\omega)$. In our experiments, we have added polystyrene particles of diameter 720 nm as tracer. Samples were filled in standard glass cuvettes (Hellma) with a path length of 5 mm and a width of 5 mm. The temperature was controlled within $\pm 0.1^\circ\text{C}$ using a temperature control chamber. A 200 mW single frequency laser (Torus 532, Laser Quantum) operating at a wavelength $\lambda = 532\text{ nm}$ was used to illuminate the sample. We collected the transmitted light using a single-mode optical fiber and single photon counting detector with high quantum efficiency and subsequently analyzed by a digital correlator. More details about the DWS device and data processing can be found in Oelschlaeger et al. [33].

2.8. $^1\text{H-NMR}$ spectroscopy

NMR experiments were performed on a Bruker NMR spectrophotometer of resonance frequency 500 MHz for ^1H -proton in D_2O .

3. Results and discussion

3.1. Gel formation and molecular interactions characterization

Several gels based on derivatives of lysine have already been reported. L-lysine hydrochloride alone cannot form gel but due to its zwitter ionic nature it can be used as bi-component gelation system. Cationic L-lysine with anionic surfactant detain solvent to gelation, this happens due to ionic interactions followed by overlapping of surfactant tail to furnish microstructure [21]. Later Adhikari et.al reported the formation of Bi-component gel composed of F-moc(L)-glutamic acid mixed with L-Lysine. The entire microstructure of these latter gels consist of an assembly of microstructures formed by cationic-anionic

interactions and π - π stacking of F-moc(L)-glutamic acid [34]. The NaTPB used in this study is reported to be slightly hydrophobic [35] while LHC is hydrophilic, as hydro-gelation occurs with the balance of hydrophilicity and hydrophobicity interactions.

Here, we developed a new strategy on the basis of previous literature cited above, where we use L-LHC and NaTPB (Scheme 1). Prior to perform mechanical and structural experiments on these gels, $^1\text{H-NMR}$ experiments (Fig. 1) have been performed on pure Lysine, pure NaTPB and on a gel of composition (1/1), total concentration 5 wt.% at temperatures of 25, 35, 50 and 90 °C. The goal is to characterize the different types of interactions present in the gel.

For the gel at 25 °C, we observe a broadening of all NaTPB and Lysine proton peaks as compared to pure molecules. This result suggests that both Lysine and NaTPB are incorporated in the gel and describes a more or less “solid-like” behavior due to restricted molecular motion [36]. Additionally, the upfield chemical shift of all NaTPB peaks suggests the presence of $\text{N-H}\cdots\pi$ type interactions between the ammonium cation of Lysine and phenyl groups of NaTPB. Numerous examples of $\text{N-H}\cdots\pi$ bonds to aromatic π systems in organic ammonium tetraphenylborates have already been reported earlier [37]. Regarding the chemical shift of Lysine peaks, this result suggests the presence of hydrogen bonding between Lysine molecules [38]. $^1\text{H-NMR}$ spectra obtained at temperatures of 35 °C and 50 °C show a similar behavior than at 25 °C but with a slight shifting of the peaks to lower values indicating that the network of the gel starts to break gradually upon increasing temperature. At 90 °C, the gel dissolves and all NaTPB and Lysine peaks sharpen again indicating the vanishing of both $\text{N-H}\cdots\pi$ and hydrogen bonding interactions. It is also important to mention that the D_2O peak occurring at ~ 4.7 ppm does not show broadening effect and no shifting indicating that water molecules are not part of the gel assembly [39]. However, crystallographic techniques and MAS NMR are required for more details about exact molecular packing. Finally, it is not excluded that beside these two types of interactions determined by NMR, i.e. $\text{N-H}\cdots\pi$ and hydrogen bonding, cationic-anionic type interactions are present. Latter presumably occur between two L-LHC molecules where one of the cationic amine group interacts with the anionic carboxylic group of another LHC molecule. A second possible interaction is between the amine group of L-LHC and the anionic borate of NaTPB. As

no gelation is observed when amine or ester groups are blocked or when cationic amine is neutralized using NaOH, latter results support the assembly hypothesis stated above.

3.2. Gel formation at constant (1/1) molar ratio: variation of the total concentration

3.2.1. Phase diagram of gels made of L-LHC and NaTPB and kinetics of formation

Instantaneous gelation occurs at room temperature when mixing aqueous solutions of L-LHC and NaTPB in an equimolar ratio at total concentrations higher than 3 wt.%. The formation of these gels has been confirmed by the inverted test tube method as well as via rheological tests. For samples below 3 wt.%, i.e. 1.5 and 2 wt.% the kinetic of gelation is much slower and takes place on a time scale of about an hour as shown by Diffusion Wave Spectroscopy (DWS) measurements (see Fig. S1 in the Supporting information file). Due to this difference in kinetic of gelation, all low concentrated gels have been investigated twenty-four hours after their preparation and high concentrated gels two hours after. Below 1.5 wt.% no gelation occurs on the investigated time scale of twenty-four hours, i.e. a minimum gelator concentration is needed for a suitable gelation.

We have also investigated the effect of pH on the gel formation using HCl and NaOH to adjust this one. At a pH range of 3–12, the gelation is instantaneous at room temperature. At very low pH (< 3), there is no gel formed; in latter case, precipitation occurs which is attributed to an instantaneous decomposition of NaTPB anion into triphenyl borane and benzene [22]. At very high pH (> 12), clear solutions are obtained due to the deprotonation of ammonium ions but no gelation occurs because α - and ϵ -amino groups of L-LHC are protected through acetylation. This result suggests that the availability of both amino groups in the L-LHC molecule is essential for gelation. Similarly, esterification of carboxyl group of L-LHC fails to gel.

3.2.2. Hydrogel Young's modulus E

Young's modulus of the gels has been determined from uniaxial compression tests as described in Section 2.5, and its variation with gelator concentration is shown in Fig. 2. The modulus adopts a power-

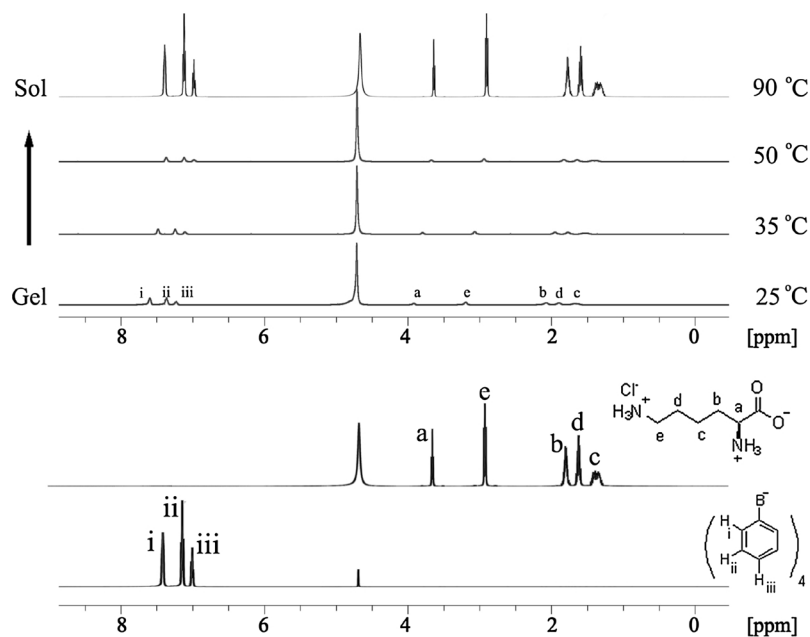


Fig. 1. $^1\text{H-NMR}$ -spectra (500 MHz) of pure NaTPB at 25 °C (bottom), pure Lysine at 25 °C (upper) and gel of composition (1/1), total concentration 5 wt.% (top) at 25 °C, 35 °C, 50 °C, 90 °C in D_2O .

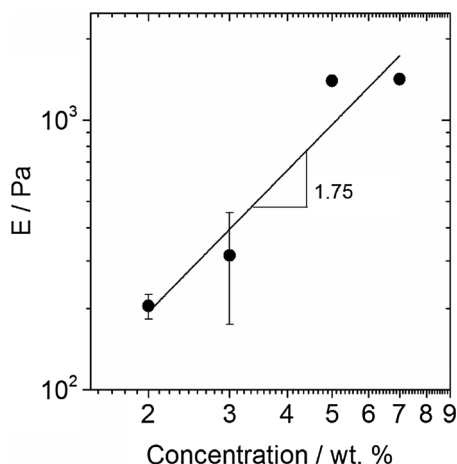


Fig. 2. Variation of the Young's modulus E as a function of total concentration for equimolar (L-LHC/NaTPB) gels.

law behavior as a function of concentration with $E \sim c^{1.75 \pm 0.25}$. Similar absolute values are obtained for the plateau modulus G_0 determined from bulk rheological measurements as will be discussed below. The concentration dependence, however, is even stronger in the latter case (see Fig. 4B). This strong increase in gel elasticity corresponds presumably to a change in the microstructure of the gel and this will be discussed later.

3.2.3. Steady state measurements

Fig. 3A shows the variation of the viscosity η as a function of the applied stress τ obtained from rotational rheometry for (1/1) gels at different concentrations. Variation of the zero-shear viscosity η_0 with gelator concentration is shown in Fig. 3B.

In Fig. 3A, two different types of flow curves are observed:

- (i) At concentrations up to 3 wt.%, we observe a pronounced shear thickening effect followed by a shear thinning regime at higher stresses. The critical stress at which shear thickening sets in increases from 1 Pa to about 10 Pa upon increasing gelator concentration from 1.5 to 3 wt.% and similarly the stress at which shear thinning starts also increases. However, the degree of shear thickening decreases with increasing gelator concentration. At 1.5 wt.% concentration, the viscosity increases by about an order of magnitude whereas this increase reduces to a factor of two at 3 wt.%.

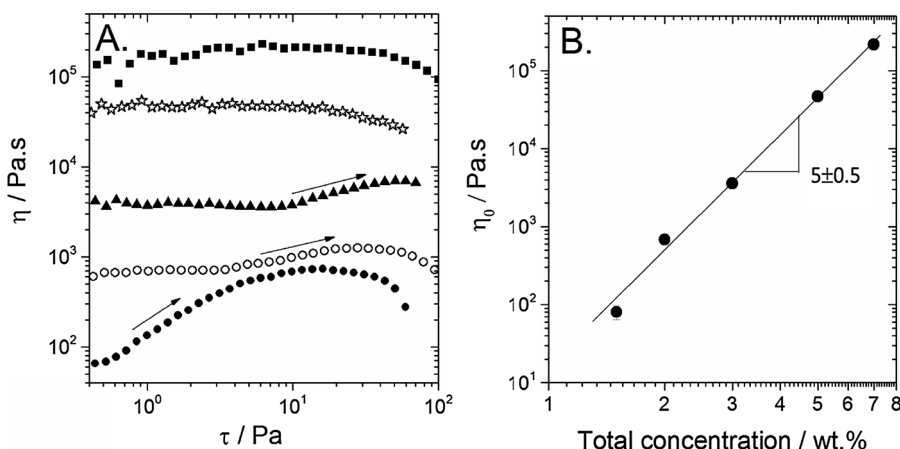


Fig. 3. (A) Variation of the viscosity η as a function of shear stress τ for equimolar (L-LHC/NaTPB) gels at total concentration of 1.5 (circle closed), 2 (star), 3 (triangle ▲), 5 (circle open) and 7 (square) wt.%. Arrows indicate the shear-thickening effect. (B) Variation of the zero-shear viscosity η_0 as a function of the total gel concentration.

- (ii) For gels at concentrations of 5 and 7 wt.% typical shear thinning flow curves are observed; i.e. at low stresses, the viscosity is constant corresponding to the value of the zero-shear viscosity and then η slightly decreases at higher stresses.

These different types of flow behavior are supposed to be related to gel structural and/or microstructural changes depending on the total gel concentration.

Irrespective to the change in non-linear flow resistance a unique power law scaling is observed, valid in the whole concentration range investigated here (see Fig. 3B). This experimental scaling exponent is much higher than theoretically predicted for polyelectrolytes in high salt limit [40], neutral polymers in good solvent [41] where $\eta_0 \sim c^{3.75}$ as well as wormlike micelles in the fast breaking limit ($\tau_{break} \ll \tau_{rep}$) where $\eta_0 \sim c^{3.6}$ [42]. Here τ_{break} and τ_{rep} are the breaking and reptation times of the micelles, respectively. On the other hand, the exponent is very close to that predicted for neutral polymer in theta solvent [43] where $\eta_0 \sim c^{14/3}$ and wormlike micelles in the slow breaking limit ($\tau_{break} \gg \tau_{rep}$) where $\eta_0 \sim c^{5.0-5.5}$ [42].

Finally, we have investigated the effect of ionic strength on gel properties by preparing a gel of composition (1/1), total concentration 5 wt.% in presence of 1.7 M NaCl. We observe higher viscosity η and plateau modulus G_0 values of about one decade for both parameters in presence of NaCl compared to values obtained for a gel of same composition but without NaCl (see Figs. S2 and S3, respectively in the supporting information file). The presence of NaCl presumably increases electrostatic interactions between the amine group of Lysine and the anion borate of NaTPB and/or between Lysine molecules themselves [44], leading to a denser packing and finally to an increase of gel viscosity and elasticity.

3.2.4. Dynamical (oscillatory) measurements

Results of frequency sweep measurements performed on (1/1) gels at three different concentrations are shown in Fig. 4A.

All samples investigated, even at low concentration of 1.5 wt.%, exhibit a gel like behavior with $G' > G''$ and the development of a quasi-plateau in G' in the investigated frequency range ($0.01 < \omega < 30 \text{ rad s}^{-1}$). From these frequency data, we have extracted the plateau modulus G_0 as the value of G' at $\omega = 0.1 \text{ rad s}^{-1}$ which corresponds to the minimum in G'' . As for η_0 , G_0 increases strongly with concentration according to a power law $G_0 \sim c^{3.4 \pm 0.35}$ from 35 Pa to 6000 Pa when the gel concentration increases from 1.5 to 7 wt.%, respectively (Fig. 4B). Contrary to the viscosity, this scaling exponent is much higher than the value predicted theoretically for all systems cited above where the variation of G_0 is always the same with $G_0 \sim c^{2.25}$ [42].

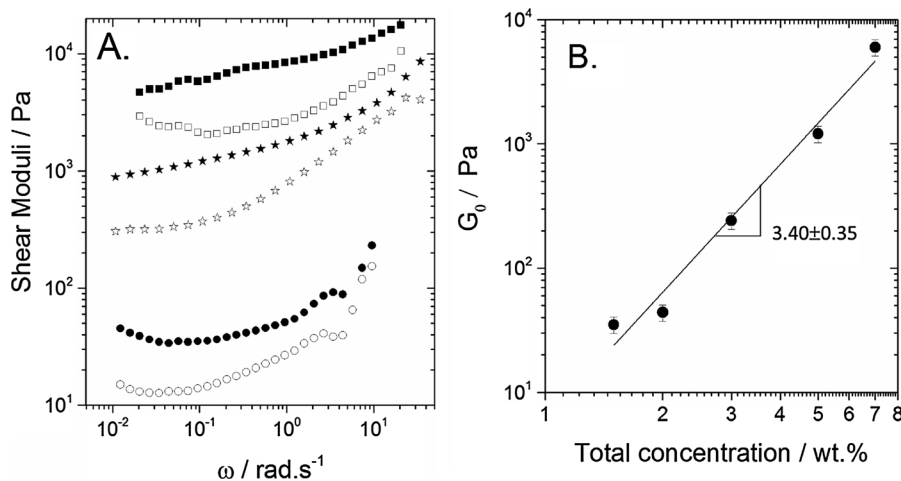


Fig. 4. Dynamic shear moduli G' (closed symbols) and G'' (open symbols) of (1/1) gels with concentrations 1.5 (circles), 5 (stars) and 7 wt.% (squares) (A). Variation of the plateau modulus G_0 (at $\omega = 0.1 \text{ rad s}^{-1}$) as a function of total gel concentration (B).

This demonstrates a strong increase in gel elasticity with increasing total concentration and this behavior can be attributed to an increase of the number of crosslinks and /or entanglements. For an ideal uniform elastic solid $E = 3G_0$. For the gels investigated here the absolute values of E and G_0 are in fair agreement but we find deviations from the simple relationship mentioned above which are most likely to be attributed to network imperfections also indicated by the noticeable values of G'' and the correspondingly low ratios $1 < G'/G'' < 10$ observed here.

3.2.5. Gel local viscoelastic properties and SEM images

We have used the multiple particle tracking technique to characterize gel structural and mechanical properties on a micrometer length scale. Typically, we have monitored the random (Brownian) motion of hundreds of embedded micron-sized particles within the fluid. From the resulting trajectories, the mean square displacement (MSD) $\langle \Delta r^2(\tau) \rangle$ of each particle has been calculated. A detailed description of this technique and the calculation procedure are shown in Mason et al. [45,46]. In our study, MPT measurements were only performed on gels at concentrations of 1.5, 2 and 3 wt.%. For more concentrated gels, particle displacements became reduced to a level similar to the so-called static error such that no reliable measurements were possible.

According to Fig. 5 at gel concentrations of 1.5 (Fig. 5A) and 2 wt.%

(Fig. 5B), MSD traces vary almost linearly with time indicating that the motion of the tracer particles is purely diffusive and that the micro-environment surrounding the particles responds like a viscous liquid. From the averaged MSD, we have determined the viscosity η_{MPT} using the relation $\langle \Delta r^2(\tau) \rangle = 4D\tau$ where the Stokes-Einstein relation gives $D = k_B T / 6\pi\eta_{MPT}a$ and a is the tracer particle radius. We found $\eta_{MPT} = 1.5 \pm 0.2$ and $1.2 \pm 0.2 \text{ mPa.s}$ for 1.5 and 2 wt.% gels respectively. These values are close to the viscosity of water ($\eta = 1 \text{ mPa s}$) indicating that the network formed at this gelator concentration has a mesh size clearly beyond $0.5 \mu\text{m}$. Additionally, for both concentrations the non-Gaussian parameter α is well below one indicating that all tracers explore a similar environment.

On the contrary, for the gel at a concentration of 3 wt.% (Fig. 5C), MSD traces are essentially time independent demonstrating that these particles are highly constrained by the surrounding solution and that they explore highly elastic regions. According to $G'_{MPT} = 2k_B T / 3\pi a \Delta r^2$ as derived by Wirtz et al. [47], we obtain a modulus $G'_{MPT} = 60 \text{ Pa}$ in reasonable agreement with bulk mechanical data (Fig. 4B). Deviations between G'_{MPT} and G_0 values may be due to some heterogeneity in gel composition also showing up in a high value for the non-Gaussian parameter $\alpha \approx 1.5$. Deeper insight into the gel structure is provided by SEM images shown in Fig. 6.

Both at gelator concentrations of 2 and 3 wt.% SEM images (Fig. 6A,

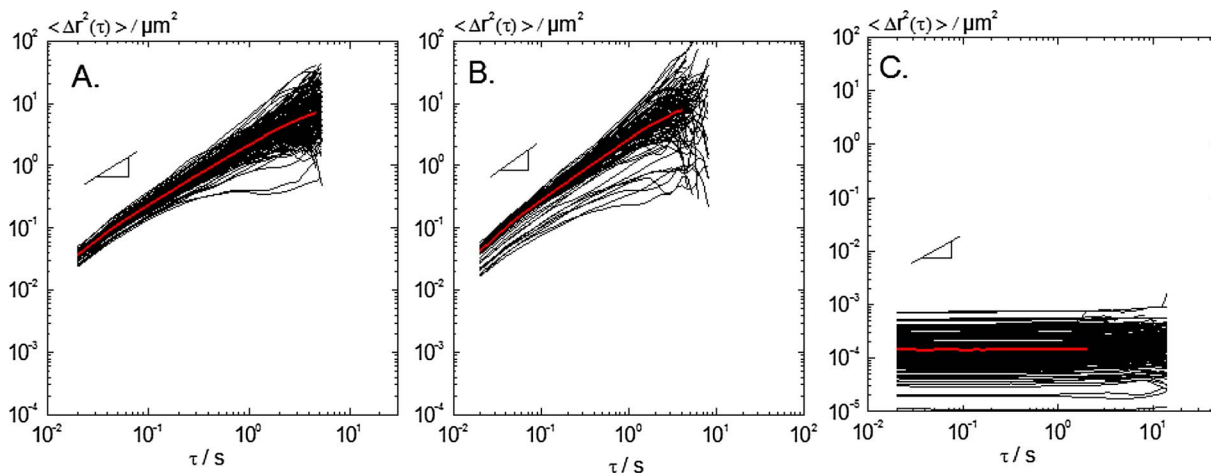


Fig. 5. MSDs of PS particles of diameter $0.5 \mu\text{m}$ dispersed in (1/1) gels of concentrations 1.5 wt.% (A), 2 wt.% (B) and of diameter $0.2 \mu\text{m}$ dispersed in a 3 wt.% (C) gel. The red curve is the ensemble-average MSD. (For interpretation of the references to red color in this figure legend, the reader is referred to the web version of this article.)

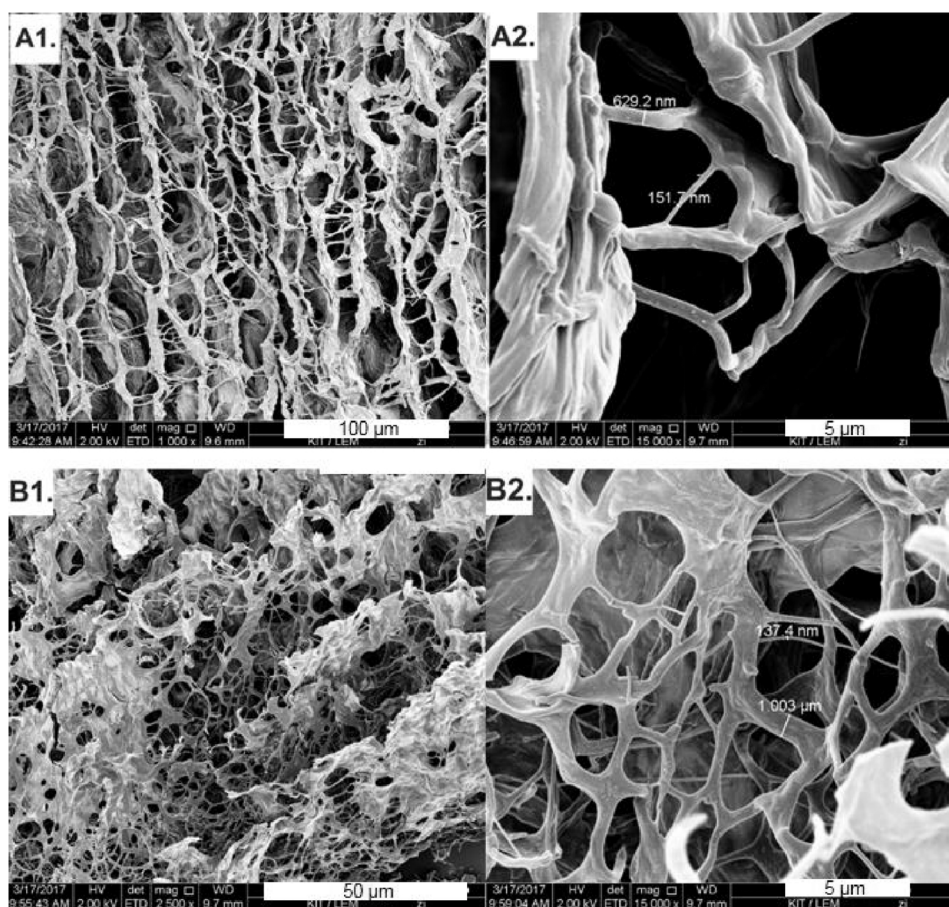


Fig. 6. Scanning electron microscope (SEM) images of (1/1) gels with concentrations of 2 wt.% (A1), and 3 wt.% (B1). (A2) and (B2) are images obtained at 15000 \times higher magnification.

B) suggest the formation of cellular structures composed of thin sheets with a constant pore size of approximately 10 μm connected via more or less thick ribbons or fibers. For the 2 wt.% gel (Fig. 6A2), these fibers have a diameter between \sim 145–600 nm whereas for the 3 wt.% gel, even 1 μm thick fibers are observed (Fig. 6B2).

In view of these SEM images, MPT measurements should then provide similar results for both 2 and 3 wt.% samples with tracer particles freely diffusing in the large pores of this structure. However, MPT discrepancies (Fig. 5B, C) may be explained by huge differences observed in the kinetics of gelation between the two samples. Indeed, for the 2 wt.% sample, the complete gelation takes \sim one hour whereas for the 3 wt.% sample, gels are formed instantaneously. Accordingly, tracer particles added in the sol state may have no time to diffuse into the pores and are trapped in the elastic sheets that form instantaneously.

A similar pore size of \approx 10 μm but a further increase in fiber diameter to $>$ 2 μm is observed for the 5 wt.% sample (Figs. 7A–C). In addition, numerous small isometric objects 250–300 nm in diameter occur decorating the fibers (Fig. 7D). These small particles may emerge from a secondary gelation process but further investigations are necessary to confirm their origin. Finally, at 7 wt.% gelator concentration (Fig. 8) a decrease of pore size to about 5 μm is observed and now the fiber diameter reduces to \approx 400 nm.

In conclusion, the unique microstructure with its porous sheets interconnected by fibers controls the viscoelastic features of the investigated gels. In particular, the strong increase in G_0 much more pronounced than for uniform entanglement networks in polymer or wormlike micelles solutions seems to be controlled by this unique structure. First, the modulus increases due to increasing thickness of fibers connecting sheets and then at 7 wt.% due to a denser packing of sheets, corresponding to a drop in mesh size.

3.3. Variation of the gel composition

3.3.1. Rotational rheology

Not only the total gel concentration has an influence on bulk rheological properties but also the gel composition as shown by flow curves obtained for samples with constant gelator concentration of 5 wt.% but different molar ratios $\frac{[\text{LHC}]}{[\text{LHC}] + [\text{NaTPB}]}$ (Fig. 9A). The gel with composition (1/10), i.e. with more NaTPB in it, shows a slight shear thickening effect whereas the (1/1) gel exhibits a typical shear thinning behavior. As for (3/1) and (1/3) gels, the viscosity is almost independent in the stress range investigated. The zero-shear viscosity varies non-monotonically with the molar ratio and exhibits a pronounced maximum $\eta_0 \approx$ 50,000 Pa s close to $\frac{[\text{LHC}]}{[\text{LHC}] + [\text{NaTPB}]} = 0.5$ and no gelation is observed at molar ratios $>$ 0.75 (Fig. 9B). A similar dependence on molar ratio is found for the plateau modulus G_0 as obtained from small amplitude oscillatory shear experiments.

3.3.2. Microrheological properties and SEM images

3.3.2.1. Compositions (1/3) and (1/10) below the viscosity maximum. Results of MPT measurements performed on samples with composition (1/3) are shown in Fig. 10. As for the sample with composition (1/1) only concentrations of 1.5, 2 and 3 wt.% have been investigated. In the 1.5 wt.% sample (Fig. 10A) tracer particles diffuse freely in a Newtonian environment, whereas the time independent MSDs found for the 3 wt.% sample (Fig. 10B) correspond to a highly elastic environment with $G_{\text{MPT}} \sim$ 15 Pa. These results are similar to what was found for the samples with molar ratio (1/1) (see Fig. 5).

Tracer particles moving freely are presumably located in large

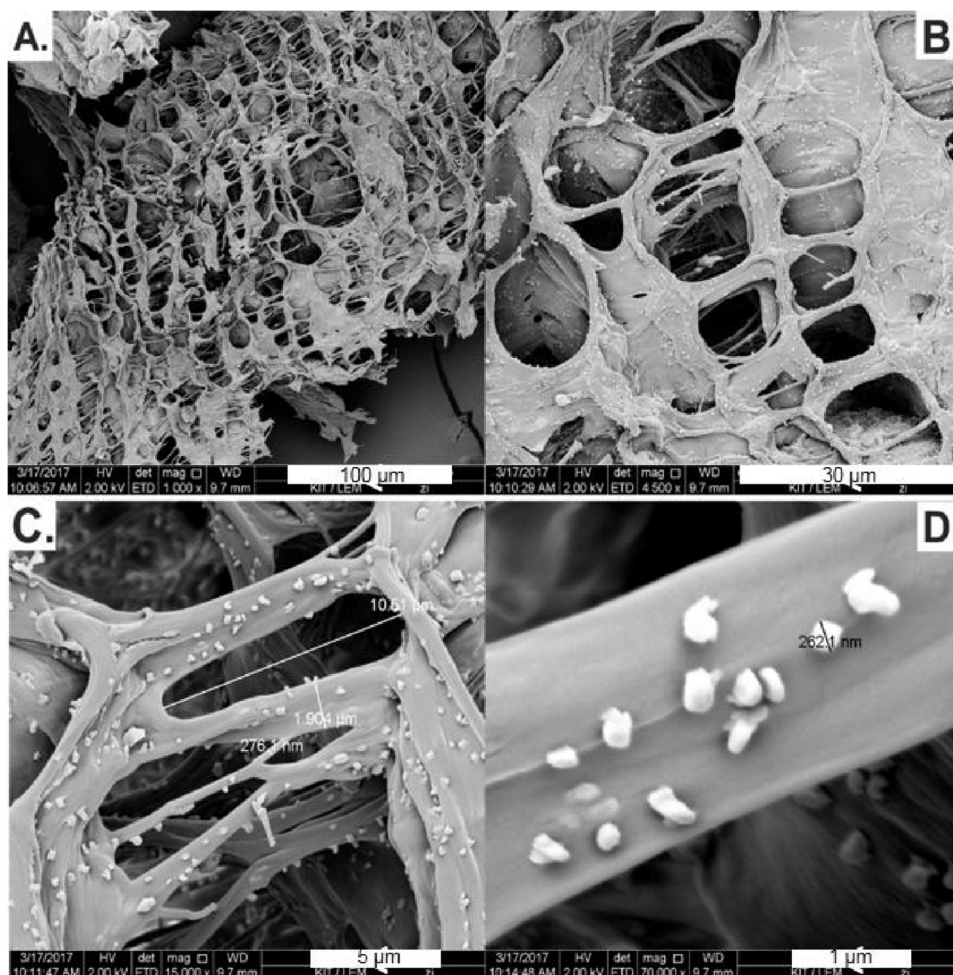


Fig. 7. (left): SEM images of a (1/1) gel with concentration of 5 wt.%. (A): Sheets with pores, (B): sheets interconnectivity, (C): Diameter of cavities between sheets and ribbons. (D): Diameter of broken fibers.

viscous areas between sheets whereas particles with restricted mobility are trapped in highly elastic sheets or fibers that form instantaneously in 3 wt.% gelator concentration irrespective of molar ratio. For the 2 wt.% sample, we have investigated different locations on the same set and have found three different types of behavior from liquid to gel-like (Figs. 10C–E). This indicates a strong heterogeneity of the structure due to the presence presumably of sheets, fibers and pores. SEM images

performed on a (1/3) sample at a concentration of 5 wt.% are shown in Fig. 11. We observe the formation of a similar structure as observed for the 5 wt.% sample with (1/1) molar ratio. The sheets seem to be thinner than in the latter case but always with a fibrillar connection.

This result supports the idea that it is NaTPB that is responsible for the formation of fibrils through N–H...π or cationic-anionic interactions and L-LHC for the formation of sheets through hydrogen bonds or

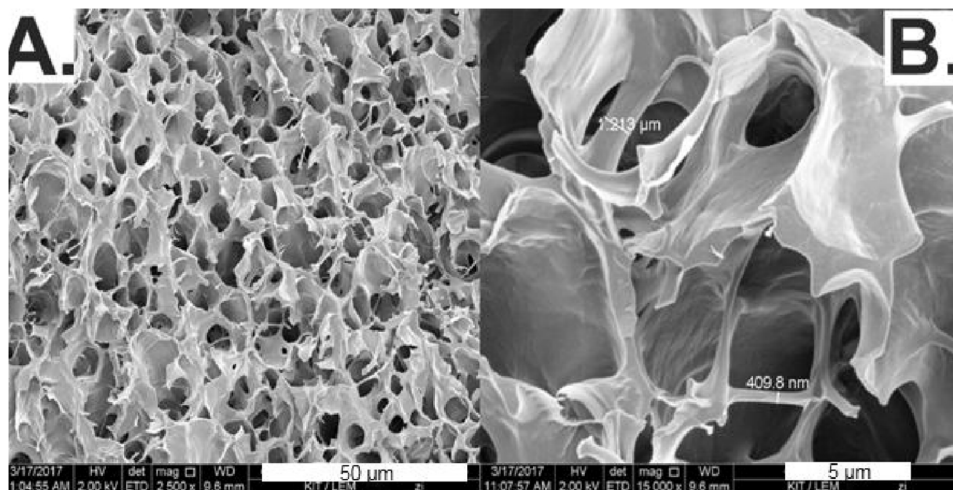


Fig. 8. (top): SEM images of a (1/1) gel with concentration of 7 wt.%. (A) Sheets with pores, dense structure highly interconnected. (B) Sheets interconnectivity.

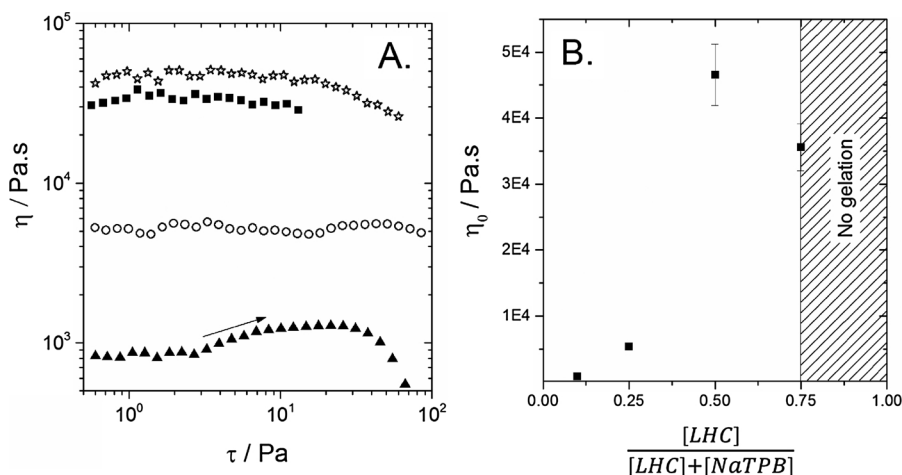


Fig. 9. (A) Variation of the viscosity η as a function of stress τ for gels with ratio (1/1) (\star), (3/1) (\blacksquare), (1/3) (\circ) and (1/10) (\blacktriangle) at constant concentration of 5% wt.%. The arrow indicates the shear-thickening effect. (B). Variation of η_0 as a function of the molar ratio $\frac{[LHC]}{[LHC] + [NaTPB]}$ for a total concentration of 5 wt.%.

cationic-anionic interactions between Lysine molecules. Thus, the low viscosity at molar ratio (1/3) is presumably due to the weaker sheet structure. For gels with even more NaTPB, molar ratio (1/10), the sheet structure is lost and a network of thick fiber bundles or agglomerates is found (Fig. 12) apparently resulting in a further viscosity drop. Another effect that can also contribute to the viscosity decrease is the ionic strength as discussed previously. Latter decreases as the stoichiometric

ratio between Na^+ and Cl^- ions deviates from the ideal (1/1) ratio leading to a reduction of the electrostatic interactions compared to the gel of composition (1/1).

3.3.2.2. Compositions (3/1) above the viscosity maximum. MPT results performed for molar ratio (3/1) at concentrations of 1.5, 2 and 3 wt.% are shown in Fig. 13.

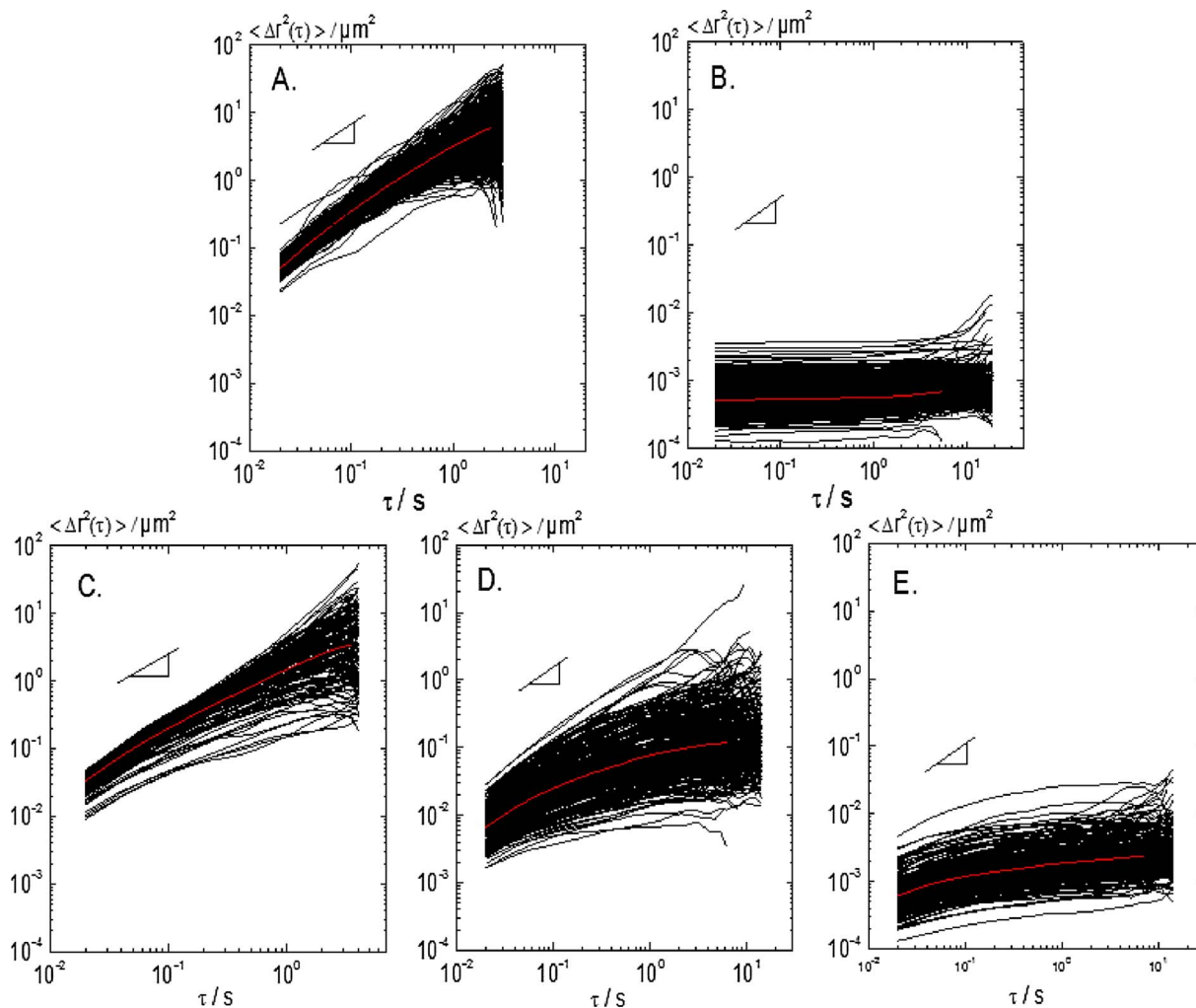


Fig. 10. MSDs of PS particles of diameter 0.5 μm dispersed in (1/3) gels of concentrations 1.5 wt.% (A), 2 wt.% (C, D, E) and of diameter 0.2 μm dispersed in a 3 wt.% (B) gel. The red curve is the ensemble-average MSD. (For interpretation of the references to red color in this figure legend, the reader is referred to the web version of this article.).

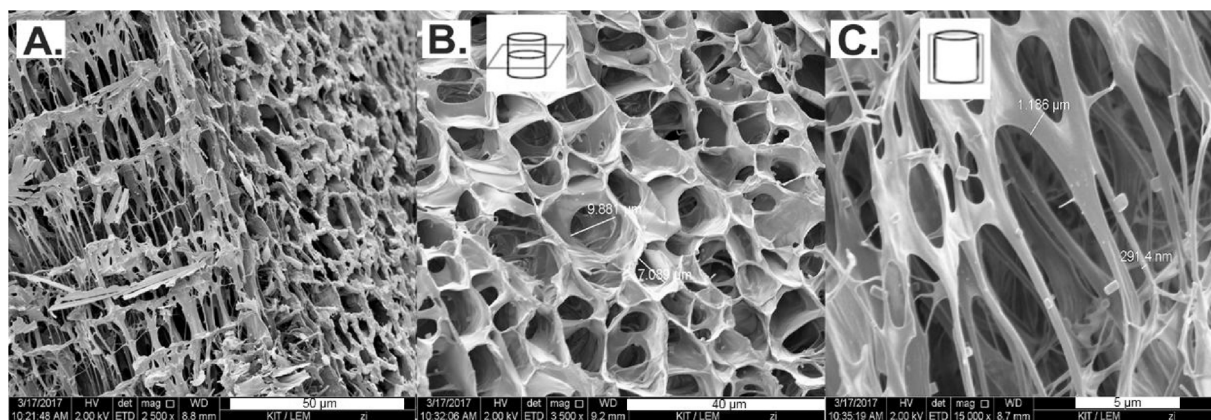


Fig. 11. Scanning electron microscope (SEM) images of a (1/3) gel with concentration of 5 wt.%. (A) low magnification. (B) Higher magnifications cross section (B) and side view (C).

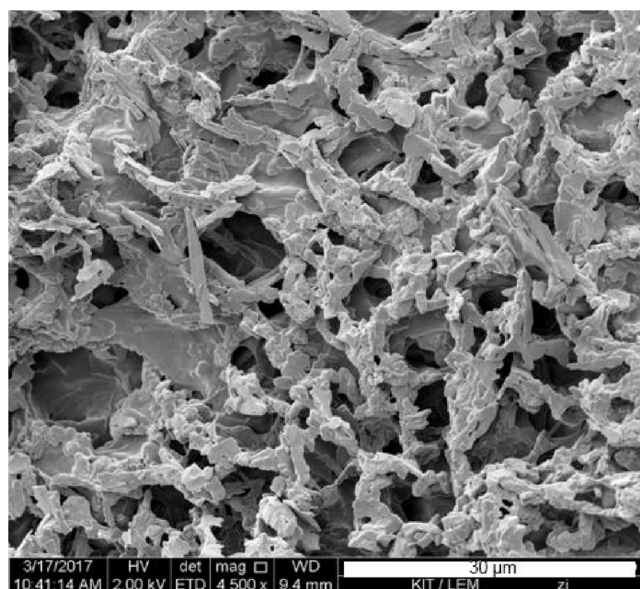


Fig. 12. Scanning electron microscope (SEM) image of a (1/10) gel with concentrations of 5 wt.%.

At 1.5 wt.% total gelator concentration two populations of tracer particles are found, one of freely diffusing particles apparently exploring a pre-dominantly viscous environment and another one of

particles for which the MSD approaches a constant limiting value at long times; these latter particles are exposed to a mainly elastic surrounding. Accordingly, the MSD at a given lag time shows a broad distribution with $\alpha = 2$. For the 2 wt.% system all tracers are trapped in an elastic environment and the shear modulus $G_{MPT} \approx 20$ Pa is in the same range as the bulk shear modulus (see Fig. 4B). These findings are clearly different from the results observed for the corresponding (1/1) systems. This indicates that the higher molar ratio of Lysine to borate results in a denser structure and as mentioned previously latter is presumably due to hydrogen bonds or cationic-anionic interactions between Lysine molecules. For the 3 wt.% system tracer particles are again exploring an elastic environment. But the absolute value of the average MSD is somewhat higher than for the corresponding equimolar system and the upturn of the MSD curves at long times indicates a finite relaxation time not observed for the (1/1) system. Accordingly, we again propose a significant microstructural change upon variation of molar ratio at constant total gelator concentration.

Obviously, the structure is distinctly different from what was observed at lower lysine to borate ratio and looks like a coral reef (Fig. 14).

3.3.3. Effect of temperature on dynamical and structural properties

We have investigated the effect of temperature on dynamical and structural properties based on diffusing wave spectroscopy (DWS) measurements performed on samples with different lysine to borate ratio. For the sample of composition (1/1), the decay of the intensity autocorrelation function (ICF) with lag time τ measured at different

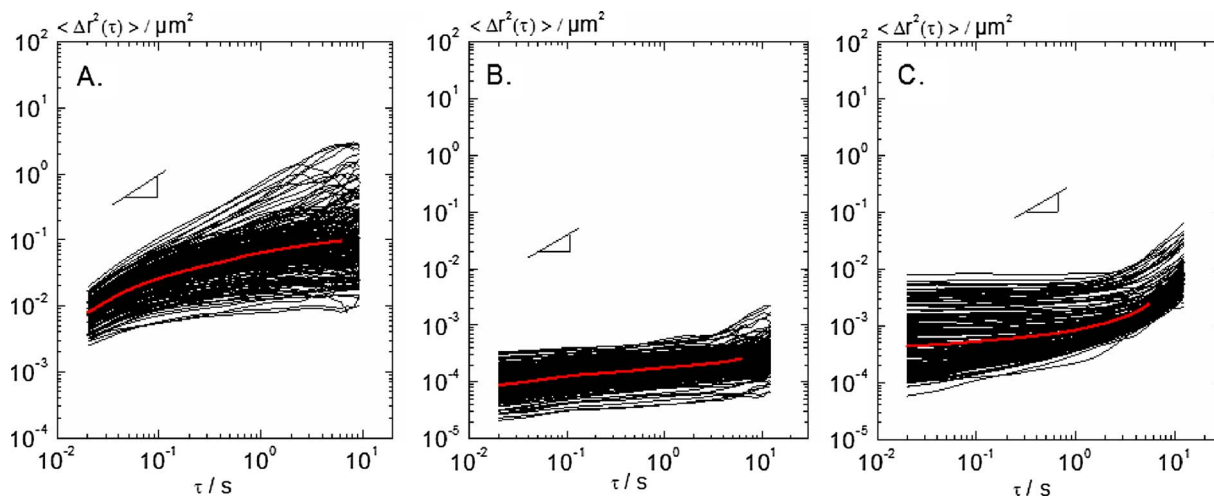


Fig. 13. MSDs of PS particles of diameter 0.5 μm dispersed in (3/1) gels of concentrations 1.5 wt.% (A), 2 wt.% (B) and of diameter 0.2 μm dispersed in a 3 (C) wt.% gel. The red curve is the ensemble-average MSD. (For interpretation of the references to red color in this figure legend, the reader is referred to the web version of this article.)

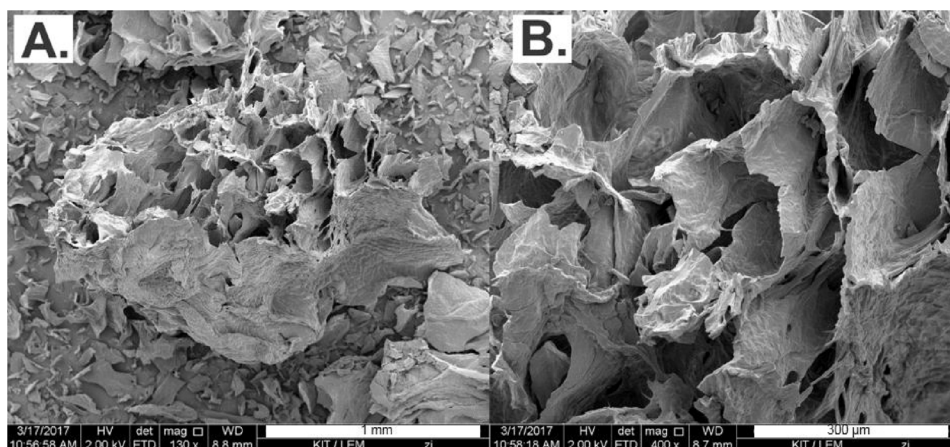


Fig. 14. Scanning electron microscope (SEM) images of a (3/1) gel with concentration of 5 wt.% at two different magnifications.

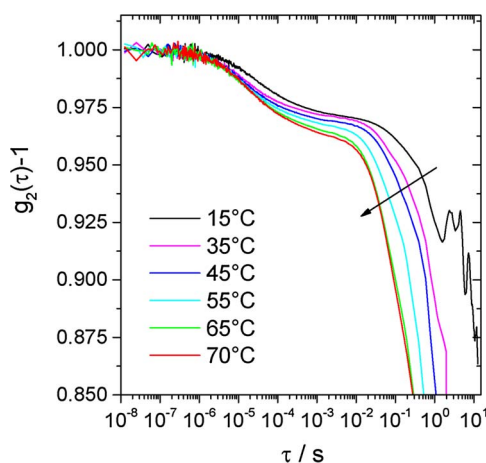


Fig. 15. Enlarge of the variation of the intensity autocorrelation function (ICF) as a function of lag time τ at different temperatures between 15 and 70 °C for a (1/1) gel with total gelator concentration of 5 wt.%. (For interpretation of the references to color in this figure legend, the reader is referred to the web version of this article.)

temperatures between 15 and 70 °C is shown in Fig. 15. For a better visualization, the left y-axis has been scaled from 1 to 0.85 instead of showing the whole decay down to zero.

The first ICF decay occurring at short times around 10^{-5} s corresponding to the diffusion of the tracer particles in the solvent as well as the pseudo-plateau developed at intermediate times

10^{-4} s $<$ τ $<$ 10^{-2} s corresponding to the trapping of the particles in the sample “network” are essentially temperature-independent. This latter result means that the elasticity of the system as characterized by the plateau modulus G_0 is almost independent of temperature. On the contrary, the second ICF decay occurring at longer times ($\tau > 10^{-2}$ s) corresponding to long range particle diffusion and marking the onset of the terminal relaxation regime indicates a strong temperature-dependency. In that latter case, the ICF decreases faster as the temperature increases from 15 to 70 °C, as showed by the arrow in Fig. 15, and indicates a decrease of the terminal relaxation time T_R . Similar results have been obtained for samples with lysine to borate ratio (1/3) and (3/1).

4. Conclusion

In this study, we have designed new low molecular weight bi-component L-Lysine-Sodium tetraphenyl borate based hydrogels with well-defined structural and mechanical features. Beside cationic-anionic molecular interactions, $^1\text{H-NMR}$ experiments have shown the

presence of N–H $\cdots\pi$ interactions as well as hydrogen bonds stabilizing the supramolecular structure.

In particular, we have shown that for equimolar ratio of lysine to borate increasing the total gelator concentration leads to a strong increase of both zero-shear viscosity and plateau modulus. For the zero-shear viscosity, this increase is similar to that predicted for neutral polymer in theta solvent or wormlike micelles in the slow breaking regime whereas for the plateau modulus it is unexpectedly higher than all predictions. SEM images as well as MPT measurements support the formation of cellular structure composed of thin sheets interconnected by fibers. Increasing the gel concentration first leads to the formation of thick fibers and then to denser sheets, which make the gels more elastic and stable.

Additionally, we have observed that gel properties can be tuned by changing their composition. For samples at constant gel concentration of 5 wt.%, increasing the lysine concentration leads to the formation of a viscosity maximum with the (1/1) equimolar composition being the optimal one. At low lysine (higher NaTPB) concentration, below the viscosity maximum, the thickness and density of the sheets decrease but with always the presence of fibrillary connections. On the other hand, at higher lysine (lower NaTPB) concentration, after the viscosity maximum, denser and thicker sheets are built but with less pore formed. These results suggest that Lysine is responsible for the formation of the sheets through hydrogen bonds or cationic-anionic interactions between Lysine molecules whereas NaTPB is responsible for the fibers formation through N–H $\cdots\pi$ or cationic-anionic interactions between NaTPB and Lysine. Finally, diffusing wave spectroscopy measurements on samples with different lysine to borate ratio revealed, that the plateau modulus G_0 is almost independent of temperature whereas the relaxation time T_R becomes faster as the temperature increases.

All these variations in morphology and mechanical properties have been performed without addition of co-solvent, salt or any other molecules. This makes this bi-component system more versatile for wide applications in soft materials sciences. For example, it can be a potential candidate as scaffolds for application in tissue engineering or can be used as a template for nano-particle synthesis. Finally, as this gel is stress responsive and electrically conductive in nature it can also be a good candidate for somato-tactile sensors.

Acknowledgments

The authors thank Tim Siebert (Institute of Process Engineering in Life Sciences, KIT Germany) and Volker Zibat (Laboratory for Electron Microscopy, KIT Germany) for their help in the cryo-SEM measurements and Ahmed Bari (King Saud University) for performing $^1\text{H-NMR}$ experiments. They also thank Shoaib Muhammad (University of Karachi) for his assistance in literature survey. Support for this work

was by Higher Education Commission (HEC) of Pakistan under project No. 20-1056/R&D/07.

Appendix A. Supplementary data

Supplementary material related to this article can be found, in the online version, at doi:<https://doi.org/10.1016/j.colsurfa.2018.02.068>.

References

- [1] D.K. Smith, Molecular gels—nanostructured soft materials, *Org. Nanostruct.* (2008) 111–154.
- [2] S.S. Babu, V.K. Praveen, A. Ajayaghosh, Functional π -gelators and their applications, *Chem. Rev.* 114 (4) (2014) 1973–2129.
- [3] K.Y. Lee, D.J. Mooney, Hydrogels for tissue engineering, *Chem. Rev.* 101 (7) (2001) 1869–1880.
- [4] T.R. Hoare, D.S. Kohane, Hydrogels in drug delivery: progress and challenges, *Polymer* 49 (8) (2008) 1993–2007.
- [5] N.A. Peppas, K.B. Keys, M. Torres-Lugo, A.M. Lowman, Poly (ethylene glycol)-containing hydrogels in drug delivery, *J. Controlled Release* 62 (1) (1999) 81–87.
- [6] H. Basit, A. Pal, S. Sen, S. Bhattacharya, Two-component hydrogels comprising fatty acids and amines: structure, properties, and application as a template for the synthesis of metal nanoparticles, *Chem.-Eur. J.* 14 (21) (2008) 6534–6545.
- [7] A.R. Hirst, B. Escuder, J.F. Miravet, D.K. Smith, High-tech applications of self-assembling supramolecular nanostructured gel-phase materials: from regenerative medicine to electronic devices, *Angew. Chem. Int. Ed.* 47 (42) (2008) 8002–8018.
- [8] S. Saha, J. Bachl, T. Kundu, D.D. Díaz, R. Banerjee, Amino acid-based multi-responsive low-molecular weight metallohydrogels with load-bearing and rapid self-healing abilities, *Chem. Commun.* 50 (23) (2014) 3004–3006.
- [9] R. Pamies, K. Zhu, A.-L. Kjøniksen, B. Nyström, Thermal response of low molecular weight poly-(N-isopropylacrylamide) polymers in aqueous solution, *Polym. Bull.* 62 (4) (2009) 487–502.
- [10] A.R. Hirst, D.K. Smith, Two-component gel-phase materials—highly tunable self-assembling systems, *Chem.-Eur. J.* 11 (19) (2005) 5496–5508.
- [11] J. Majumder, P. Dastidar, An easy access to organic salt-based stimuli-responsive and multifunctional supramolecular hydrogels, *Chem. Eur. J.* 22 (27) (2016) 9267–9276.
- [12] P. Sahoo, I. Chakraborty, P. Dastidar, Reverse thermal gelation of aromatic solvents by a series of easily accessible organic salt based gelators, *Soft Matter* 8 (9) (2012) 2595–2598.
- [13] A. Ballabh, D.R. Trivedi, P. Dastidar, Ascertaining the 1D hydrogen-bonded network in organic ionic solids, *Cryst. Growth Des.* 5 (4) (2005) 1545–1553.
- [14] D.R. Trivedi, P. Dastidar, Instant gelation of various organic fluids including petrol at room temperature by a new class of supramolecular gelators, *Chem. Mater.* 18 (6) (2006) 1470–1478.
- [15] D.R. Trivedi, A. Ballabh, P. Dastidar, Supramolecular assemblies in salts and co-crystals of imidazoles with dicarboxylic acids, *Cryst. Eng. Comm.* 5 (64) (2003) 358–367.
- [16] M. George, R.G. Weiss, Chemically reversible organogels: aliphatic amines as “Latent” gelators with carbon dioxide, *J. Am. Chem. Soc.* 123 (42) (2001) 10393–10394.
- [17] A. Darabi, P.G. Jessop, M.F. Cunningham, CO₂-responsive polymeric materials: synthesis, self-assembly, and functional applications, *Chem. Soc. Rev.* 45 (2016) 4391–4436.
- [18] C. Manohar, U. Rao, B. Valaulikar, R. Lyer, On the origin of viscoelasticity in micellar solutions of cetyltrimethylammonium bromide and sodium salicylate, *J. Chem. Soc. Chem. Commun.* 5 (1986) 379–381.
- [19] H. Katano, T. Yoneoka, N. Kito, C. Maruyama, Y. Hamano, Separation and purification of *D*-poly-L-lysine from the culture broth based on precipitation with the tetraphenylborate anion, *Anal. Sci.* 28 (12) (2012) 1153–1157.
- [20] J. Lin, Q. Tang, J. Wu, S. Hao, The synthesis and electrical conductivity of a polyacrylate/graphite hydrogel, *React. Funct. Polym.* 67 (4) (2007) 275–281.
- [21] Y.I. González, E.W. Kaler, Fibrous assemblies and water gelation in mixtures of lysine with sodium alkyl sulfates, *Langmuir* 21 (16) (2005) 7191–7199.
- [22] M. Suzuki, K. Hanabusa, L-Lysine-based low-molecular-weight gelators, *Chem. Soc. Rev.* 38 (4) (2009) 967–975.
- [23] J.M. Paulusse, D. Van Beek, R.P. Sijbesma, Reversible switching of the sol–gel transition with ultrasound in rhodium (I) and iridium (I) coordination networks, *J. Am. Chem. Soc.* 129 (8) (2007) 2392–2397.
- [24] L. Chen, J. Raeburn, S. Sutton, D.G. Spiller, J. Williams, J.S. Sharp, P.C. Griffiths, R.K. Heenan, S.M. King, A. Paul, Tuneable mechanical properties in low molecular weight gels, *Soft Matter* 7 (20) (2011) 9721–9727.
- [25] J.A. Foster, R.M. Edkins, G.J. Cameron, N. Colgin, K. Fucke, S. Ridgeway, A.G. Crawford, T.B. Marder, A. Beeby, S.L. Cobb, Blending gelators to Tune gel structure and probe anion-induced disassembly, *Chem.-Eur. J.* 20 (1) (2014) 279–291.
- [26] M. Chau, K.J. DeFrance, B. Kopera, V.R. Machado, S. Rosenfeldt, L. Reyes, K.J. Chan, S. Förster, E.D. Cranston, T. Hoare, Composite hydrogels with tunable anisotropic morphologies and mechanical properties, *Chem. Mater.* 28 (10) (2016) 3406–3415.
- [27] S. Naser, C. Bechinger, P. Leiderer, T. Palberg, Finite-size effects on the closest packing of hard spheres, *Phys. Rev. Lett.* 79 (12) (1997) 2348.
- [28] A. Kowalczyk, C. Oelschlaeger, N. Willenbacher, Tracking errors in 2D multiple particle tracking microrheology, *Meas. Sci. Technol.* 26 (1) (2014) 015302.
- [29] J.C. Crocker, D.G. Grier, Methods of digital video microscopy for colloidal studies, *J. Colloid Interface Sci.* 179 (1) (1996) 298–310.
- [30] L. Van Hove, Correlations in space and time and Born approximation scattering in systems of interacting particles, *Phys. Rev.* 95 (1) (1954) 249.
- [31] E.R. Weeks, J.C. Crocker, A.C. Levitt, A. Schofield, D.A. Weitz, Three-dimensional direct imaging of structural relaxation near the colloidal glass transition, *Science* 287 (5453) (2000) 627–631.
- [32] C. Oelschlaeger, F. Bossler, N. Willenbacher, Synthesis, structural and micro-mechanical properties of 3D hyaluronic acid-based cryogel scaffolds, *Biomacromolecules* 17 (2) (2016) 580–589.
- [33] C. Oelschlaeger, M. Schopferer, F. Scheffold, N. Willenbacher, Linear-to- branched micelles transition: a rheometry and diffusing wave spectroscopy (DWS) study, *Langmuir* 25 (2009) 716–723.
- [34] B. Adhikari, J. Nanda, A. Banerjee, Multicomponent hydrogels from enantiomeric amino acid derivatives: helical nanofibers, handedness and self-sorting, *Soft Matter* 7 (19) (2011) 8913–8922.
- [35] W. Kleijn, L. Bruner, M. Midland, J. Wisniewski, Hydrophobic ion probe studies of membrane dipole potentials, *Biochim. Biophys. Acta (BBA)* 727 (2) (1983) 357–366.
- [36] M. Tata, V.T. John, Y.Y. Waguespack, G.L. McPherson, Microstructural characterization of novel phenolic organogels through high-resolution NMR spectroscopy, *J. Phys. Chem.* 98 (14) (1994) 3809–3817.
- [37] P.K. Bakshi, A. Linden, B.R. Vincent, S.P. Roe, D. Adhikesavalu, T.S. Cameron, O. Knop, Crystal chemistry of tetra-radial species. Part 4. Hydrogen bonding to aromatic π systems: crystal structures of fifteen tetraphenylborates with organic ammonium cations, *Can. J. Chem.* 72 (5) (1993) 1273–1293.
- [38] J.H. Jung, S. Shinkai, T. Shimizu, Spectral characterization of self-assemblies of aldopyranoside amphiphilic gelators: what is the essential structural difference between simple amphiphiles and bolaamphiphiles? *Chem. Eur. J.* 8 (12) (2002) 2684–2690.
- [39] H. Basit, A. Pal, S. Sen, S. Bhattacharya, Two-component hydrogels comprising fatty acids and amines: structure, properties, and application as a template for the synthesis of metal nanoparticles, *Chem. Eur. J.* 14 (21) (2008) 6534–6545.
- [40] A.V. Dobrynin, R.H. Colby, M. Rubinstein, Scaling theory of polyelectrolyte solutions, *Macromolecules* 28 (6) (1995) 1859–1871.
- [41] P.-G. De Gennes, *Scaling Concepts in Polymer Physics*, Cornell university press, 1979.
- [42] M. Cates, Dynamics of living polymers and flexible surfactant micelles: scaling laws for dilution, *J. Phys.* 49 (9) (1988) 1593–1600.
- [43] R.H. Colby, Structure and linear viscoelasticity of flexible polymer solutions: comparison of polyelectrolyte and neutral polymer solutions, *Rheol. Acta* 49 (2010) 425–442.
- [44] B. Ozbas, J. Kretsinger, K. Rajagopal, J.P. Schneider, D.J. Pochan, Salt-triggered peptide folding and consequent self-assembly into hydrogels with tunable modulus, *Macromolecules* 37 (19) (2004) 7331–7337.
- [45] T.G. Mason, D. Weitz, Optical measurements of frequency-dependent linear viscoelastic moduli of complex fluids, *Phys. Rev. Lett.* 74 (7) (1995) 1250.
- [46] T. Mason, K. Ganesan, J. Van Zanten, D. Wirtz, S. Kuo, Particle tracking microrheology of complex fluids, *Phys. Rev. Lett.* 79 (17) (1997) 3282.
- [47] D. Wirtz, Particle-tracking microrheology of living cells: principles and applications, *Annu. Rev. Biophys.* 38 (2009) 301–326.